

## Relay sliding mode control based on the input-output model

Şölen KUMBAY YILDIZ\*, Hüseyin DEMİRCİOĞLU

Department of Electrical and Electronics Engineering, Hacettepe University, Ankara, Turkey

Received: 13.03.2014

Accepted/Published Online: 17.10.2014

Final Version: 15.04.2016

**Abstract:**Uncertainties, parameter changes, and disturbances lie among the most frequently encountered problems in practical control applications. Sliding mode control (SMC) is one of the robust control methods developed to provide a certain control performance under such circumstances. SMC can also be achieved in relay control systems. The aim is to obtain an overall system that is robust to disturbances, noise, and parameter changes by forcing the relay element to operate in sliding mode. While SMC methods have been traditionally developed in state-space, in relay control systems, it is possible to define SMC based on the input-output model of a system. This way, sliding motion can be achieved by only utilizing the output signal, without the need to know or measure the system states.

In this study, the relay sliding mode control method based on the input-output model proposed in previous studies is revisited. Sliding conditions under ideal operating conditions are reformulated to fortify the theoretical background. Some additional issues, namely the effects of disturbances and measurement noise on the sliding mode conditions, are addressed and analyzed in detail. Finally, the theoretical results are put to the test by detailed simulation examples.

**Key words:** Sliding mode control, robust control, relay control, input-output model, RSMC-IO

### 1. Introduction

Variable structure systems (VSS) and sliding mode control (SMC) methods have been widely studied since their emergence in the 1970s [1–3], resulting in a significant number of publications in the literature. The reader is referred to [4–9] for some basic and detailed information regarding this approach. SMC still attracts a significant amount of interest from researchers, mainly due to the fact that it provides a very robust control performance under the influence of uncertainties, parameter changes, and disturbances.

The basic idea of SMC is to vary the structure of the system by switching between two or more different structures and forcing the system state to move along a predetermined manifold that determines the desired closed-loop behavior of the overall system. The resulting behavior is called sliding motion and the manifold is usually referred to as the sliding manifold or sliding surface. The price being paid for the robust control performance is the phenomenon called chattering, which is caused by the discontinuous nature of the control action. Chattering often leads to undesirable results such as energy losses, low control accuracy, wearing of mechanical parts, and excitation of unmodeled dynamics. Various solutions to reduce the chattering problem have been proposed in the literature, such as replacing the discrete control action by a continuous function, adjusting the control signal adaptively to decrease its amplitude, or filtering the control signal by a low-pass filter before applying it to the system [10–14].

Traditionally, the design of SMC methods has been dominated by the state-space representation; as a

\*Correspondence: solen@ee.hacettepe.edu.tr

result, the sliding surface is defined as a function of system states. Hence, the system states need to be either measured or observed [15–17]. Since generating estimates of unavailable internal states is a complex problem on its own, a different kind of SMC, called output feedback SMC, has been proposed in the 1990s. This method requires only output information, restricting the definition of the sliding surface to the states that are available through measured outputs [18–20].

Relay control systems are considered a type of VSSs that can be controlled using SMC methods. The objective is to force the relay element to operate in sliding mode in order to obtain a robust control performance against parameter variations and disturbances. For relay control systems, SMC design can be formulated using the input-output model, as opposed to the traditional approaches based on state-space models. The relay sliding mode control method based on the input-output model does not require any knowledge of system states; only the system's output is utilized. This approach was most likely first addressed in [21] and [22]; in these works conditions for sliding motion were given and the control performance of the proposed method was illustrated via computer simulations and real applications. A more recent study compares the relay sliding mode control method with adaptive model reference control methods [23]. While both approaches exhibit a similar performance under the influence of noise, the performance of relay sliding mode control is shown to be superior, especially when the system's parameters change rapidly.

The previous studies on relay sliding mode control based on the input-output model have mainly addressed sliding mode conditions under ideal operating conditions and the analyses appear to be incomplete. This paper is based on the recent work in [24]. Its purpose is to extend the previous works by providing a more complete formulation and thorough analysis for sliding mode conditions than those presented in previous works and address the issues of noise and disturbances, which have not been addressed before.

The paper is organized as follows: Section 2 covers the sliding mode conditions in a relay control system under ideal operating conditions. The effects of disturbances and parameter changes on the sliding mode conditions are addressed in Section 3. To demonstrate the control performance of relay sliding mode control based on the input-output model, various simulation examples are given in Section 4. Section 5 is the conclusion part.

## 2. Relay sliding mode control based on the input-output model (RSMC-IO)

Consider the block diagram of a relay control system given in Figure 1, where  $G(s)$  is the transfer function of the open-loop system and  $M(s)$  is the transfer function of the model.  $w(t)$ ,  $e(t)$ ,  $u(t)$ , and  $y(t)$  represent the set-point (or reference), relay input (also referred to as the error), control input, and closed-loop system output, respectively.  $\phi(t)$  denotes the system's output filtered with the inverse of the model.  $s$  is either the differential operator ( $d/dt$ ) or the Laplace operator depending on the context.

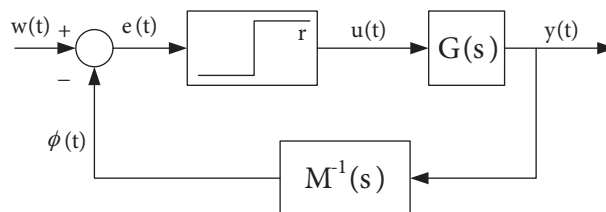


Figure 1. A relay control system.

Under the assumption that the relay is symmetric and ideal with amplitude  $r$ , the control signal can be given by

$$u(t) = r \operatorname{sign}(e(t)) = \begin{cases} r, e(t) \geq 0 \\ -r, e(t) < 0 \end{cases} \quad (1)$$

The inequality

$$e(t)\dot{e}(t) < 0 \quad (2)$$

is the necessary and sufficient condition for sliding motion to occur in this system [2,25]. In other words, when the relay input  $e(t)$  crosses the threshold ( $e(t) = 0$ ), it immediately recrosses it, resulting in sliding motion. The system is said to operate in sliding mode. Here,  $e(t) = 0$  defines the sliding surface. When in sliding mode, since  $e(t) = 0$ , the closed-loop system behavior is given by the following equations:

$$\begin{aligned} w - \phi &= 0 \\ w - M^{-1}y &= 0 \\ y &= Mw \end{aligned} \quad (3)$$

Eq. (3) states that the system's behavior is solely governed by the reference model during the sliding mode.  $M(0) = 1$  is assumed to guarantee that no steady-state error occurs. In practice, as the assumption of  $e(t) = 0$  is unrealistic, the output can be written as

$$y = Mw - Me. \quad (4)$$

Since  $e(t)$  is a signal with low amplitude and high frequency, its effect on the output will be insignificant after it is filtered with  $M(s)$ , and so the term  $Me$  can be neglected.

For the system shown in Figure 1,  $e(t)$  and  $\dot{e}(t)$  are given by the following equations (assuming  $w$  is differentiable):

$$\begin{aligned} e &= w - \phi \\ \dot{e} &= \dot{w} - \dot{\phi} \\ &= \dot{w} - sM^{-1}Gu \\ &= \dot{w} - (\beta u + \dot{\phi}^o) \\ &= \dot{w} - \beta u - \dot{\phi}^o \\ &= \dot{w} - \beta r \operatorname{sign}(e) - \dot{\phi}^o \\ \dot{e} &= \begin{cases} \dot{w} - \beta r - \dot{\phi}^o, e > 0 \\ \dot{w} + \beta r - \dot{\phi}^o, e < 0 \end{cases} \end{aligned} \quad (5)$$

Here the signal  $\dot{\phi}$  (i.e. the term  $sM^{-1}Gu$ ) is broken down into two signals,  $\beta u$  and  $\dot{\phi}^o$ ; the term  $\beta u$  denotes the instantaneous change in  $\dot{\phi}$  as a result of a change in  $u$ , and the term  $\dot{\phi}^o$  is the remaining part. The definition of  $\beta$  is given below.

$$\beta = \lim_{s \rightarrow \infty} sM^{-1}(s)G(s) \quad (6)$$

Using Eq. (5) the conditions to satisfy Eq. (2) are found as

$$\begin{aligned} \beta r &> \dot{w} - \dot{\phi}^o, e > 0 \\ \beta r &> -\dot{w} + \dot{\phi}^o, e < 0 \end{aligned} \quad (7)$$

or simply

$$\beta r > |\dot{w} - \dot{\phi}^o|. \tag{8}$$

Note that this is an improved sliding condition compared to the previous works in [21,22] and, to our knowledge, this is the first occurrence of it in SMC literature.

It is important to point out that the loop transfer function of the system shown in Figure 1 must satisfy the condition

$$\rho(M^{-1}G) = 1 \tag{9}$$

for sliding motion to occur, where  $\rho$  indicates relative order. If the relative order is  $\rho(M^{-1}G) > 1$ , then  $\beta$  will be zero and Eq. (8) cannot be satisfied. The condition in Eq. (8) also depends on the sign of  $\beta$ . If  $\beta > 0$ , it is satisfied when  $r > 0$ ; if  $\beta < 0$ , the relay needs to be reversed ( $r < 0$ ).

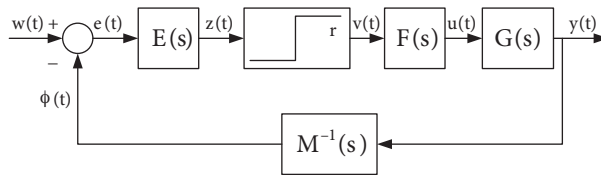


**Figure 2.** Extended structure for a relay control system.

If the relative order condition given in Eq. (9) is not satisfied for a given system and a desired model, filters of appropriate orders can be placed before and/or after the relay element, so that the relative order of the overall loop transfer function becomes 1 [21]. The resulting structure is shown in Figure 2 [23]. Here  $E(s)$  and  $F(s)$  are user defined filters, chosen to make the relative order of the loop transfer function  $E(s)M^{-1}(s)G(s)F(s)$  unity ( $\rho(EM^{-1}GF) = 1$ ). For this purpose, either only one of the filters or both may be used. In this structure, the relay input is denoted by  $z(t)$ ; therefore, the condition for the relay to operate in sliding mode becomes

$$z(t)\dot{z}(t) < 0 \tag{10}$$

and the system output is given by

$$y = Mw - \frac{M}{E}z. \tag{11}$$

Similar to the previous structure shown in Figure 1, the system's behavior during the sliding phase is dictated by the model, since  $z(t)$  is a low amplitude signal with a high frequency and the second term can be neglected. To derive the sliding mode conditions for this structure, consider the relay input and its derivative.

$$\begin{aligned} z &= E(w - \phi) \\ \dot{z} &= E(\dot{w} - \dot{\phi}) \\ &= E\dot{w} - sEM^{-1}GFv \\ &= E\dot{w} - (\beta v + \dot{\phi}^o) \\ &= E\dot{w} - \beta r \text{sign}(z) - \dot{\phi}^o \\ \dot{z} &= \begin{cases} E\dot{w} - \beta r - \dot{\phi}^o, z > 0 \\ E\dot{w} + \beta r - \dot{\phi}^o, z < 0 \end{cases} \end{aligned} \tag{12}$$

From Eq. (12), sliding mode conditions are found as

$$\begin{aligned}\beta r &> E\dot{w} - \dot{\phi}^o, z > 0 \\ \beta r &> -E\dot{w} + \dot{\phi}^o, z < 0\end{aligned}\quad (13)$$

which can also be expressed in a single inequality as

$$\beta r > |E\dot{w} - \dot{\phi}^o|. \quad (14)$$

It can be seen in Eq. (12) that the term  $sEM^{-1}GFv$  was split into two signals  $\beta v$  and  $\dot{\phi}^o$  as before, where  $\beta$  is defined as

$$\beta = \lim_{s \rightarrow \infty} sE(s)M^{-1}(s)G(s)F(s) \quad (15)$$

Once again, the sign of  $\beta$  is important. The relay amplitude  $r$  needs to be selected appropriately, so that  $\beta r$  is positive. Moreover, the relative order of the loop transfer function must satisfy the condition

$$\rho(EM^{-1}GF) = 1, \quad (16)$$

otherwise Eq. (14) cannot be satisfied. If the necessary filter to satisfy Eq. (16) consists of only derivatives, it should be chosen as  $E(s)$  and placed before the relay. Otherwise, it can be chosen as either  $E(s)$  or  $F(s)$  and can be placed before or after the relay. However, it is recommended to place it after the relay element as  $F(s)$  in order to filter out the high frequency components of the signal generated at the relay output. By doing so, the chattering problem can be alleviated and the plant is protected from rapidly changing inputs at the same time.

### 3. Robustness analysis of RSMC-IO

SMC methods are known to be robust against parameter variations and disturbances. In this section, the robustness of RSMC-IO is investigated.

#### 3.1. Parameter variations

One of the most commonly encountered problems in control applications is parameter variations, mainly caused due to the system structure or operating conditions that may change in time. As explained at the beginning of Section 2, once the sliding mode conditions are met and the system operates in sliding mode, the system's behavior becomes independent from the open-loop system and is solely dictated by the reference model (Eq. (3)). As long as the effects of these parameter variations on  $\dot{\phi}^o$  are small and the conditions in Eq. (8) hold, the control performance will not be affected. This can be assured by choosing a large enough relay amplitude  $r$ . A simulation example with varying plant parameters will be presented in Section 4.

#### 3.2. Disturbances and measurement noise

In this section, the effects of disturbance acting on the output and measurement noise on the sliding mode conditions are investigated, neither of which have been addressed in a previous study on RSMC-IO. Consider the block diagram of a relay control system shown in Figure 3, where  $n(t)$  and  $m(t)$  represent disturbance on the output and measurement noise, respectively.

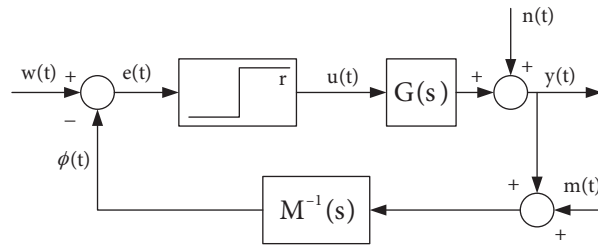


**Figure 3.** Relay control system with disturbance acting on its output and measurement noise.

Three frequently encountered types of disturbance signals are addressed in this work; these are step function, sinusoidal, and white noise.  $m(t)$  is assumed to be zero when the effect of the disturbance is investigated. From Figure 3, the error can be written as

$$\begin{aligned} e &= w - \phi \\ &= w - M^{-1}(Gu + n) , \\ &= w - M^{-1}Gu - \psi \end{aligned} \tag{17}$$

where  $\psi$  is defined as  $\psi = M^{-1}n$ . Considering the error derivative

$$\begin{aligned} \dot{e} &= \dot{w} - sM^{-1}Gu - \dot{\psi} \\ \dot{e} &= \dot{w} - (\beta r \text{sign}(e) + \dot{\phi}^o) - \dot{\psi} \\ \dot{e} &= \begin{cases} \dot{w} - \beta r - \dot{\phi}^o - \dot{\psi}, e > 0 \\ \dot{w} + \beta r - \dot{\phi}^o - \dot{\psi}, e < 0 \end{cases} \end{aligned} \tag{18}$$

sliding mode conditions are obtained as

$$\begin{aligned} \beta r &> \dot{w} - \dot{\phi}^o - \dot{\psi}, e > 0 \\ \beta r &> -\dot{w} + \dot{\phi}^o + \dot{\psi}, e < 0 \end{aligned} \tag{19}$$

or

$$\beta r > |\dot{w} - \dot{\phi}^o - \dot{\psi}|. \tag{20}$$

Eqs. (19) and (20) suggest that, depending on  $|\dot{\psi}|$ , a larger relay amplitude  $r$  might be required to satisfy the conditions to obtain sliding motion under the influence of noise when compared to the ideal case with no disturbance (see Eq. (7)). Note that the output of the system in Figure 3 is given as

$$y = Mw - Me, \tag{21}$$

which means that  $n(t)$  has no effect on the system's behavior while the system is operating in sliding mode. In other words, the system is robust against disturbance.

Assume that the disturbance is modeled as

$$n(t) = d \tag{22}$$

i.e. a step function. When the steady-state response is considered, the signal  $\psi$  and its derivative will be given as

$$\begin{aligned} \psi &= M^{-1}(0)d = d \\ \dot{\psi} &= 0. \end{aligned} \tag{23}$$

Using Eq. (23) the sliding mode condition given in Eq. (20) takes the following form:

$$\beta r > |\dot{w} - \dot{\phi}^o| \quad (24)$$

Eq. (24) states that the sliding mode conditions are the same as in the ideal case with no disturbances. However, during the transient response, that is, when the step function disturbance jumps to a new level,  $\dot{\psi}$  will be different from zero ( $\dot{\psi} \neq 0$ ) and its magnitude ( $|\dot{\psi}|$ ) will be very large. Hence, at these points in time, the inequality  $\beta r > |\dot{w} - \dot{\phi}^o - \dot{\psi}|$  may not be satisfied, but this is an instantaneous event and the condition is immediately satisfied again. At these points in time the system may move away from sliding mode, but as soon as the error reaches zero it continues to operate in sliding mode.

When the disturbance is modeled as a sinusoidal signal with amplitude  $A$  and frequency  $\omega$ , the following equations can be written:

$$\begin{aligned} n(t) &= A \sin(\omega t) \\ \dot{n}(t) &= A \omega \cos(\omega t) \\ \dot{\psi}(t) &= M^{-1} \dot{n}(t) \end{aligned} \quad (25)$$

It is clear that  $|\dot{\psi}|$  is proportional to the frequency ( $\omega$ ) of the disturbance. Hence, the higher  $\omega$  is, the larger would be the necessary relay amplitude to satisfy the condition in Eq. (20).

Modeling the disturbance signal  $n(t)$  as white noise would result in the need for an even larger relay amplitude to satisfy sliding mode conditions, since  $|\dot{\psi}|$  would be larger when compared to the sinusoidal noise model. Studies have shown that this relay amplitude is usually too large, which makes it impossible or impractical to be realized in real applications. As seen in Figure 3, the output  $y$  is filtered with the inverse of the model  $M^{-1}$ . To filter out the high frequency components of the noise, the inverse of the model transfer function can be modified as

$$M'^{-1}(s) = \frac{M^{-1}(s)}{D(s)}, \quad (26)$$

where  $M(s)$  is the actual model and  $D(s)$  is the filter polynomial. The bandwidth of the filter  $1/D(s)$  must be properly chosen to eliminate the unwanted effects of the noise.  $M'(s)$  is now the modified model including the filter. It is important to point out that the steady-state gain of the modified model transfer function is kept as  $M'(0) = 1$ . With the introduction of  $D(s)$  into the model, the relative order condition given in Eq. (9) is no longer maintained. At higher frequencies where  $n(t)$  is more effective,  $D(s)$  will be chosen such that

$$\frac{1}{D(j\omega)} \approx 0 \Rightarrow M'^{-1}(j\omega) \approx 0. \quad (27)$$

However, at lower frequencies, such as the operating frequency of the plant,  $D(s)$  will be chosen as

$$\frac{1}{D(j\omega)} \approx 1 \Rightarrow M'^{-1}(j\omega) \approx M^{-1}(j\omega) \quad (28)$$

According to Eqs. (27) and (28) the relative order conditions cannot be maintained at high frequencies, but they can still be maintained at lower frequencies and thus it is possible to obtain sliding motion. This way, a small relay amplitude can be found to satisfy the sliding mode condition given in Eq. (20).

To assess the effect of measurement noise on the sliding mode conditions, consider the system in Figure 3. This time the disturbance at the output is assumed to be zero ( $n(t) = 0$ ). Writing the error and its derivative as

$$\begin{aligned} e &= w - \phi \\ &= w - M^{-1}(y + m) \\ &= w - M^{-1}Gu - M^{-1}m \\ &= w - M^{-1}Gu - \mu \end{aligned} \tag{29}$$

and

$$\begin{aligned} \dot{e} &= \dot{w} - sM^{-1}Gu - \dot{\mu} \\ &= \dot{w} - \beta u - \dot{\phi}^o - \dot{\mu} \\ &= \dot{w} - \beta r \text{sign}(e) - \dot{\phi}^o - \dot{\mu} \\ \dot{e} &= \begin{cases} \dot{w} - \beta r - \dot{\phi}^o - \dot{\mu}, e > 0 \\ \dot{w} + \beta r - \dot{\phi}^o - \dot{\mu}, e < 0 \end{cases}, \end{aligned} \tag{30}$$

where  $\mu$  is defined as  $\mu = M^{-1}m$ , results in the sliding mode conditions given below.

$$\left. \begin{aligned} \beta r > \dot{w} - \dot{\phi}^o - \dot{\mu}, e > 0 \\ \beta r > -\dot{w} + \dot{\phi}^o + \dot{\mu}, e < 0 \end{aligned} \right\} \Rightarrow \beta r > |\dot{w} - \dot{\phi}^o - \dot{\mu}| \tag{31}$$

Note that the inequalities given in Eq. (31) are similar to those in Eq. (19). However, considering the output during the sliding phase (i.e. when  $e = 0$ )

$$\begin{aligned} w - M^{-1}(y + m) &= 0 \\ y &= Mw - m \end{aligned} \tag{32}$$

it is obvious that the measurement error is added directly to the output signal. In other words, while SMC is robust to parameter changes and disturbances on the output signal, it is sensitive to measurement noise, a fact that is often disregarded in SMC literature. Hence, the choice of the sensory equipment plays an important role in the control performance of RSMC-IO.

Considering disturbance and measurement noise together, the general conditions for sliding motion are given as

$$\left. \begin{aligned} \beta r > \dot{w} - \dot{\phi}^o - \dot{\psi} - \dot{\mu}, e > 0 \\ \beta r > -\dot{w} + \dot{\phi}^o + \dot{\psi} + \dot{\mu}, e < 0 \end{aligned} \right\} \Rightarrow \beta r > |\dot{w} - \dot{\phi}^o - \dot{\psi} - \dot{\mu}| \tag{33}$$

#### 4. Simulations

To demonstrate the performance of RSMC-IO, some simulation examples are presented in this section. The simulations were performed using MATLAB running on a personal computer. The sampling interval is chosen as 1ms.

The system and model considered in the first group of examples are

$$G_1(s) = \frac{1}{s^2 + s + 1}, M_1(s) = \frac{1}{0.25s + 1}. \tag{34}$$



Note that the relative order of the closed loop system is  $\rho(M_1^{-1}G_1) = 1$  and  $\beta$  can be calculated as  $\beta = 0.25$ . Since  $\beta$  is positive, a positive relay amplitude is required to satisfy the sliding mode conditions given in Eq. (7). Simulation results with  $r = 3$  are provided in Figure 4. Here the first graph includes the set-point  $w$  (sinusoidal wave), the model output  $y_m$  (dashed line), and the system response  $y$  (solid line). The control input  $u$ , i.e. the relay output, is plotted in the second graph and the relay input (error)  $e$  is given in the third graph. The third graph also includes the signal  $|\dot{w} - \dot{\phi}^o|$  and the term  $\beta r$ . It is clear that the condition  $\beta r > |\dot{w} - \dot{\phi}^o|$  holds during the entire simulation. Therefore, the error is zero at all times and the relay output is oscillating between  $\pm r$  at high frequency. In other words, the relay is operating in sliding mode. Note that the system output tracks the model perfectly in Figure 4.a.

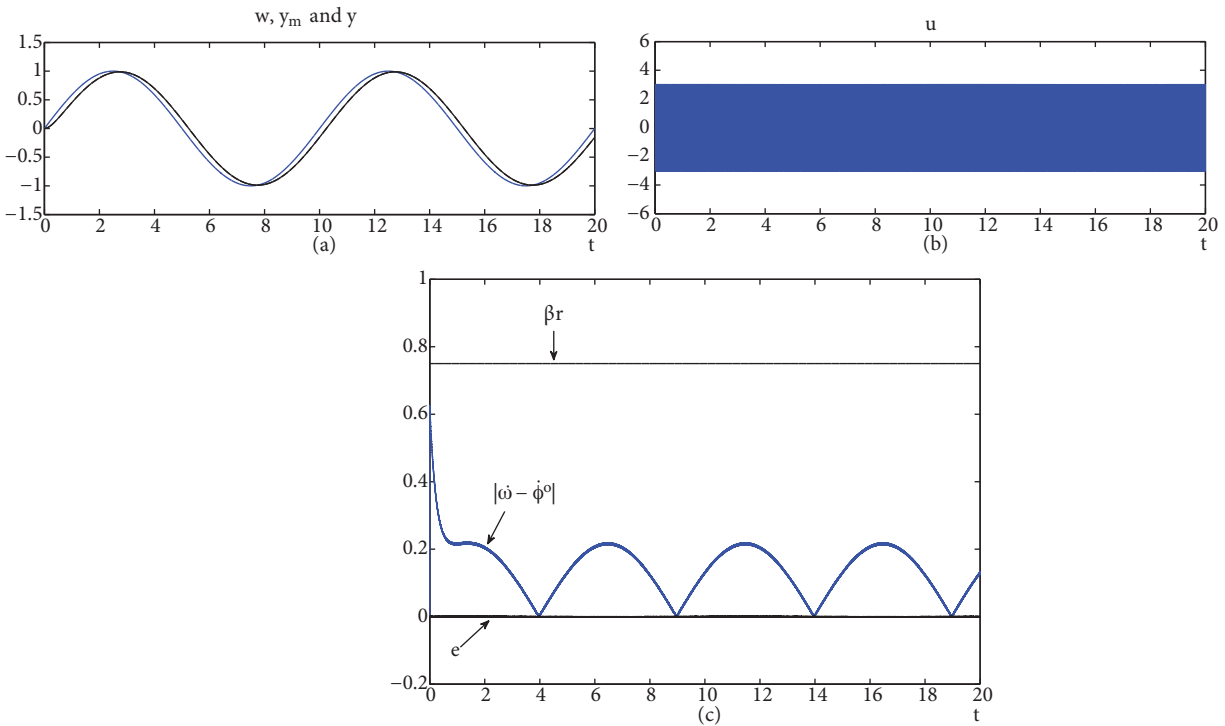


**Figure 4.** Simulation results for  $G_1(s)$  and  $M_1(s)$  with  $r = 3$ .

In order to illustrate what happens when the sliding mode conditions are not satisfied at certain times, the system in Eq. (34) is simulated with  $r = 0.8$  and the results are given in Figure 5. While the first two graphs show the same signals as in the previous example, the third graph includes the signal  $\dot{w} - \dot{\phi}^o$  when the error is positive ( $e > 0$ ) and  $-\dot{w} + \dot{\phi}^o$  when  $e$  is negative ( $e < 0$ ). As seen from the figure, the system is not in sliding mode throughout all the simulation time; instead, at certain times it is not operating in sliding mode. Figure 5.a shows that model tracking is not achieved until  $t \approx 4s$ . The control input is observed to be constant at  $u = r = 0.8$  in the first few seconds of the run (Figure 5.b). This behavior can be easily understood by examining Figure 5.c. At the start of the simulation the error is positive and increasing, i.e. the necessary condition for sliding motion ( $e\dot{e} < 0$ ) is not satisfied. Consequently, the condition  $\beta r > \dot{w} - \dot{\phi}^o$  is also not met (see Eq. (7)). This condition is satisfied at  $t \approx 1.3s$ , at which point the error is still positive but decreasing, i.e.  $e\dot{e} < 0$ . As soon as the error signal reaches  $e = 0$  the relay starts operating in sliding mode and the system output begins to track the response of the model. This behavior continues until  $t \approx 6s$  when Eq. (7) no longer

holds and the error becomes negative and decreasing (i.e.  $e\dot{e} > 0$ ). As a result, the relay stops operating in sliding mode and the input signal takes the value  $u = -r = -0.8$ , since  $e < 0$ . At  $t \approx 7.5s$ , the condition  $\beta r > -\dot{w} + \dot{\phi}^o$  is satisfied and the error starts increasing. When the error reaches  $e = 0$  sliding motion is achieved again until the next instant when the conditions in Eq. (7) are no longer satisfied. It is essential to point out that the purpose of this example was to demonstrate the system's behavior when the relay amplitude is not sufficiently large. Since this is not the intended or the preferred way of implementing the RSMC-IO method, the relay amplitudes in the remaining examples given in this section will be chosen large enough to satisfy the sliding mode conditions.

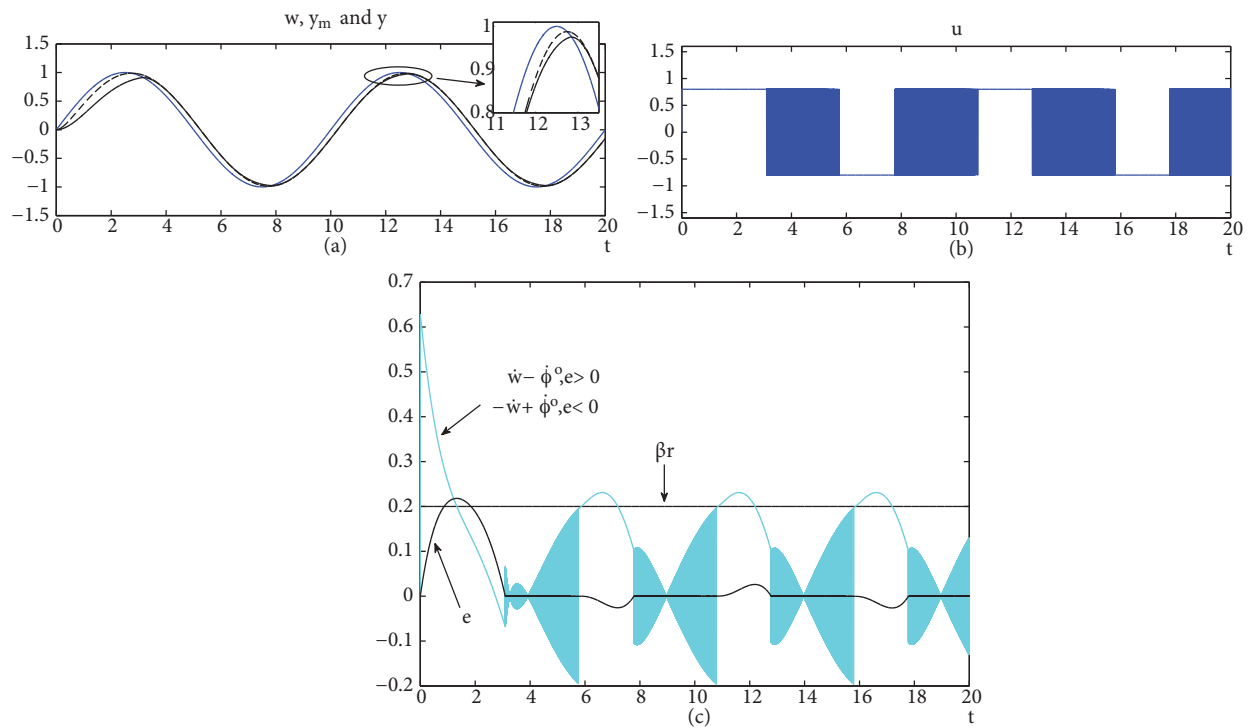


**Figure 5.** Simulation results for  $G_1(s)$  and  $M_1(s)$  with  $r = 0.8$ .

From this point on, the reference signals in the simulations are in the form of a square wave, a type of signal that is widely used in practical applications. The simulation results for the system in Eq. (34) using a square wave set-point are presented in Figure 6. The results show that the condition  $\beta r > |\dot{w} - \dot{\phi}^o|$  is met throughout the simulation except the instances at which the value of the set-point changes. At these instances the signal  $|\dot{w}|$  takes a very large value; therefore, a larger relay amplitude is required to maintain the sliding mode condition, which is usually impossible or impractical to realize in practice. Note that the sliding mode condition is disrupted for only an instant and it is satisfied again, and so the error reaches  $e = 0$ . Recall that the value of the relay amplitude determines the duration of the reaching phase. As the relay amplitude is increased, the duration of the reaching phase becomes shorter. Figure 6.a indicates that perfect model following is achieved during the steady state. Model following during the transient phase can be improved by further increasing the relay amplitude.

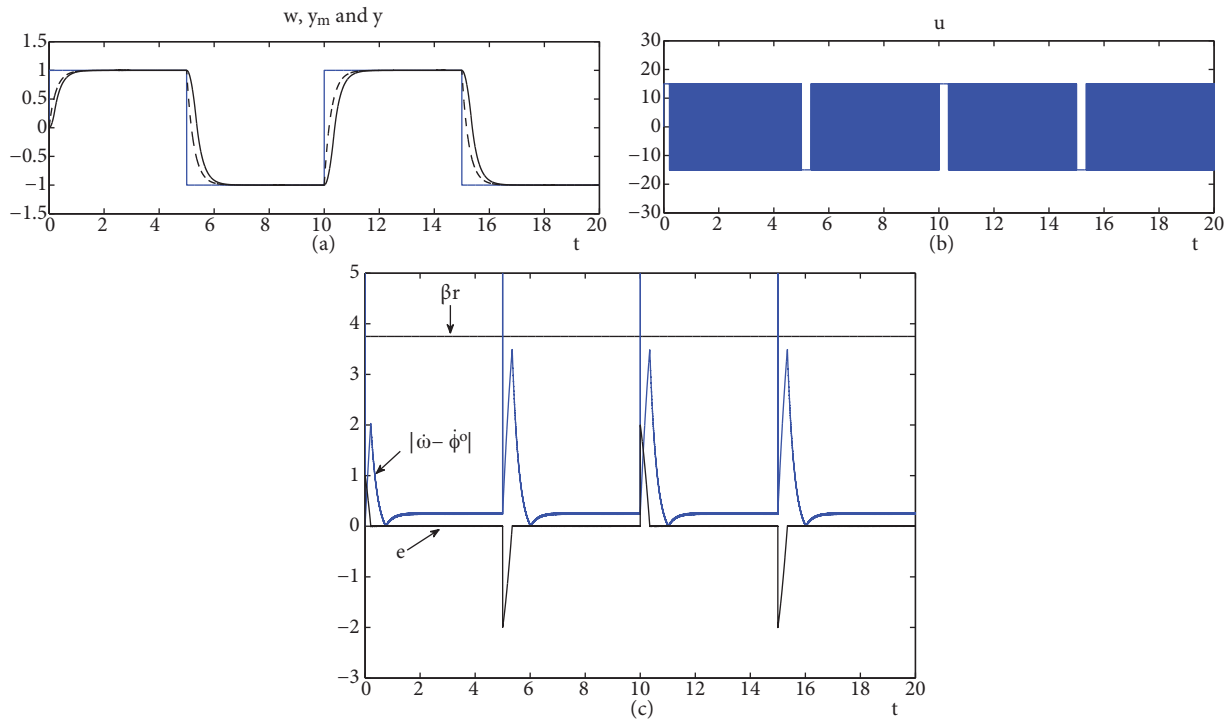


Figure 6. Simulation results for  $G_1(s)$  and  $M_1(s)$  with  $r = 15$ .

The examples presented so far have confirmed the accuracy of the sliding mode conditions derived in Section 2. Simulations carried out using a sinusoidal reference signal indicate that the system operates in sliding mode over the course of the entire run as long as a sufficiently large relay amplitude is chosen. Sliding motion stops and the control performance deteriorates whenever the conditions in Eq. (7) are not met. Similar to the sinusoidal case, a large enough relay amplitude assures a good control performance when a square wave is used as reference. Sliding motion is only interrupted when the set-point jumps to another value, provided that Eq. (8) is satisfied during the remaining time of the run. The relay amplitude determines the duration of the reaching phase after a set-point change. Therefore, the aim is to determine a large enough relay amplitude for sufficiently short reaching phases.

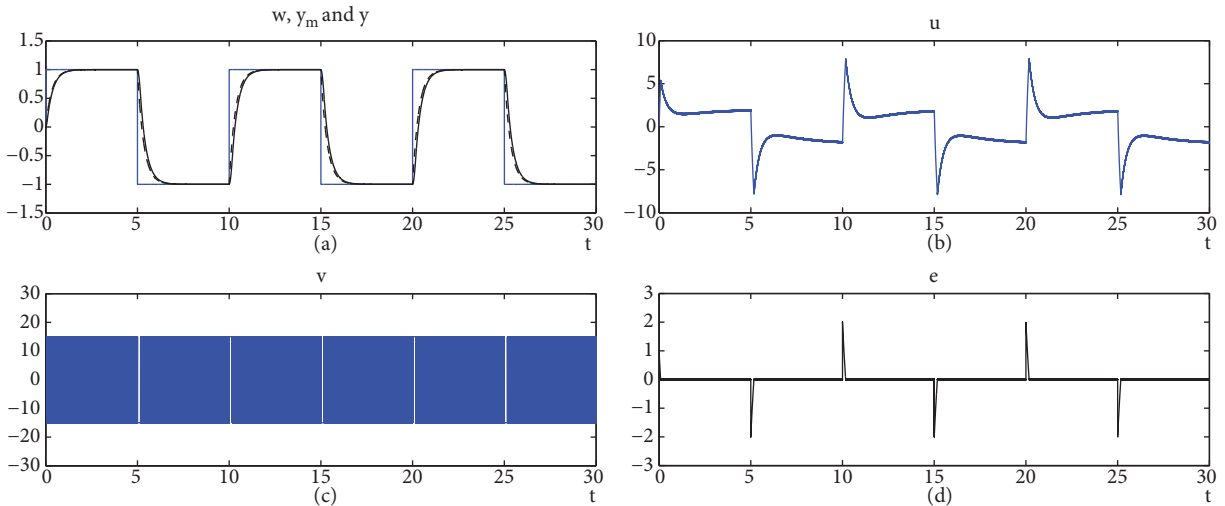
To summarize, the condition  $\beta r > |\dot{w} - \dot{\phi}^o|$  is essential for sliding motion to occur. If this condition is satisfied for all  $t \geq 0$ , the system starts operating in sliding mode from the beginning. For this scenario, the sliding mode condition can also be expressed as  $\beta r > \sup|\dot{w} - \dot{\phi}^o|$ . The term  $\beta r$  is expected to be as large from the term  $|\dot{w} - \dot{\phi}^o|$  as possible. Since  $\beta$  is constant for a given system, it is concluded that  $|r|$  has to be sufficiently large.

Two simulations are presented next to provide examples for the use of the filters  $E(s)$  and  $F(s)$  covered in Section 2. The first of these simulations was carried out using the system and model in Eq. (35).

$$G_2(s) = \frac{s + 0.5}{2s^2 + 2s + 1}, M_2(s) = \frac{1}{\frac{1}{3}s + 1}, F(s) = \frac{1}{0.2s + 1} \tag{35}$$

Here the relative order of the loop transfer function is  $\rho(M_2^{-1}G_2) = 0$ . Since the condition in Eq. (9) is not satisfied, a filter  $F(s)$  is used. The relative order of the resulting loop transfer function becomes

$\rho(M_2^{-1}G_2F) = 1$ , satisfying the condition in Eq. (16). The simulation results presented in Figure 7 consist of four graphs. As in the previous examples, the first graph shows the set-point  $w$  (square wave), the model output  $y_m$  (dashed line), and the system response  $y$  (solid line), and the second graph shows the control input  $u$ . Note that this system has the extended structure shown in Figure 2. Therefore, the control input is no longer the signal at the output of the relay, but the filtered version of it by  $F(s)$ . The relay output  $v$  is plotted in the third graph and the relay input (error)  $e$  can be seen in the last graph. The relay amplitude is chosen as  $r = 15$ . It can be observed that initially the error is positive but reaches  $e = 0$  quickly. It stays at  $e = 0$  and the relay keeps operating in sliding mode until the set-point changes. The sliding mode conditions are satisfied at every point in time except when the set-point jumps to another value. The system starts operating in sliding mode after short reaching phases, since the relay amplitude is chosen large enough. Aside from satisfying the relative order condition, the filter  $F(s)$  leads to a smoother control input by filtering out the high frequency components of the relay output; hence the chattering problem is also overcome. Model following is successfully achieved as is evident in Figure 7.a.



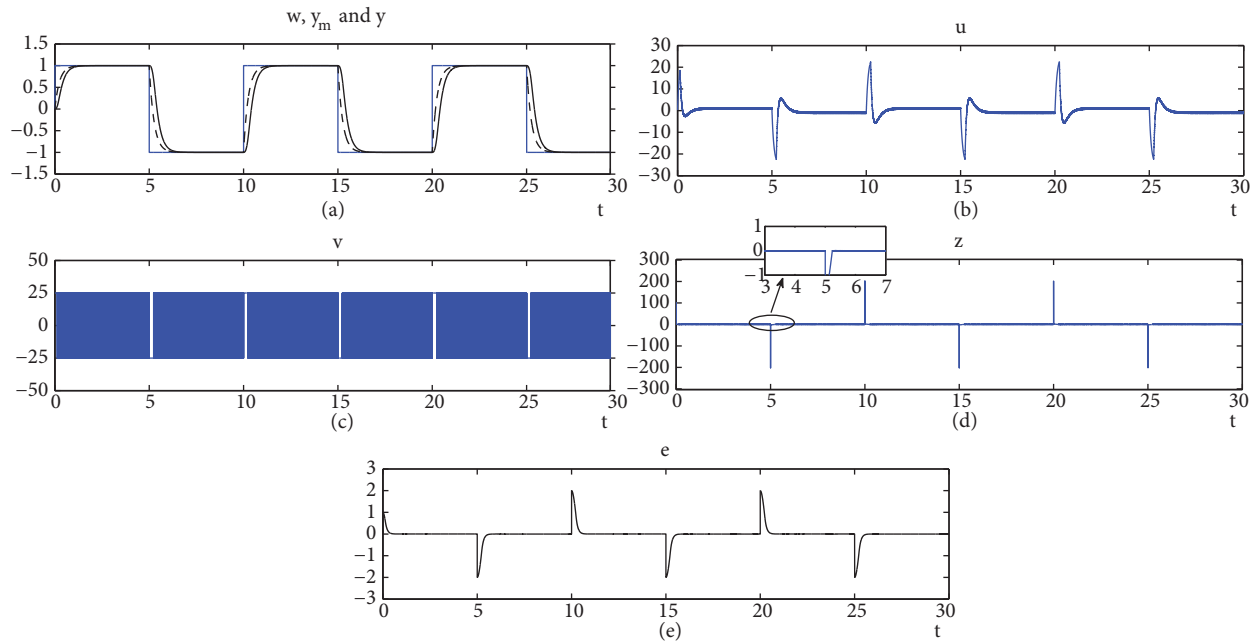
**Figure 7.** Use of filter  $F(s)$ . Results for  $G_2(s)$  and  $M_2(s)$  with  $r = 15$ .

Figure 8 provides the results of a simulation carried out using the system and model in Eq. (34). Although the loop transfer function satisfies the relative order condition ( $\rho(M_1^{-1}G_1) = 1$ ), the aim here is to obtain a smoother control input in order to eliminate the chattering problem. For this purpose the filters in Eq. (36) were utilized.

$$E(s) = 0.1s + 1, F(s) = \frac{1}{0.1s + 1} \tag{36}$$

The relative orders of the filters  $E(s)$  and  $F(s)$  were chosen appropriately to ensure that the condition in Eq. (16) is met ( $\rho(EM_1^{-1}G_1F) = 1$ ). In Figure 8, the first three graphs are similar to the previous figure. In the fourth graph the relay input  $z$  is shown and  $e$  is plotted in the fifth graph. The relay amplitude is determined as  $r = 25$ . Note that  $z$  is a signal with high frequency and low amplitude oscillating around zero. As a result, the relay is operating in sliding mode and model following is achieved.

It is important to emphasize that, in the last two examples, the relay elements are not used as actuators. Instead, the control inputs are obtained by filtering the relay outputs with  $F(s)$ . Therefore, physical limitations



**Figure 8.** Use of filters  $E(s)$  and  $F(s)$ . Results for  $G_1(s)$  and  $M_1(s)$  with  $r = 25$ .

on the actuators are no longer relevant for the choice of the relay amplitude and as a result larger relay amplitudes can be chosen when compared to the case when the relay is used as the actuator element.

It is a well-known fact that parameters of a system are usually not constant and may change in time, mainly due to variations in operating conditions and uncertainties in the system structure. The following example aims to demonstrate the performance of RSMC-IO under such circumstances. The system and model given in Eq. (35) are considered. The transfer function of the plant can be shown as

$$G_2(s) = \frac{s + 0.5}{2s^2 + 2s + 1} = \frac{s + 0.5}{a_2s^2 + a_1s + a_0} \quad (37)$$

The changes in the values of the plant parameters during the simulation are as follows: at  $t = 17$   $a_1$  is instantaneously changed from  $a_1 = 2$  to  $a_1 = 4$ . The parameters  $a_0$  and  $a_2$  are arranged to vary sinusoidally as  $a_0(t) = 1 + \sin(2\pi t/T_0)$  and  $a_2(t) = 2 + \sin(2\pi t/T_2)$  with  $T_0 = 5s$  and  $T_2 = 25s$  throughout the simulation. The simulation results with  $r = 5$  are shown in Figure 9. The signals  $\dot{w} - \dot{\phi}^o$ ,  $-\dot{w} + \dot{\phi}^o$  and the product  $\beta r$  are plotted alongside the error. The set-point jumps set aside, this graph shows that the parameter variations do not disrupt the sliding mode conditions. Since the system structure is constantly changing due to the variations in the system parameters, the resulting control action is not repeated in each period like in previous examples. Moreover, the durations of the reaching phases that occur after set-point changes are different from each other as a result of the dynamical system structure. The relay stops operating in sliding mode at  $t = 17s$  for a short time because the error takes a negative value due to the sudden parameter change. Since the sliding mode condition holds, the error returns to  $e = 0$  after a reaching phase and sliding motion occurs again. The results of this simulation confirm that RSMC-IO performs well when the system's parameters are not constant, as long as the sliding mode conditions are not disrupted. This can be achieved by choosing an appropriate relay amplitude.

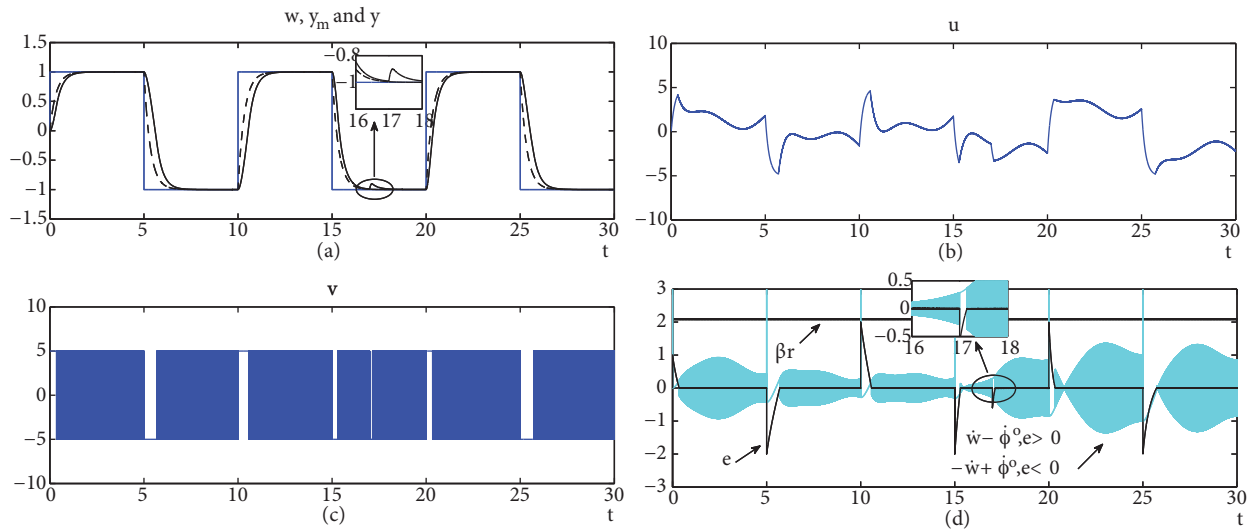


**Figure 9.** Parameter variations. Results for  $G_2(s)$  and  $M_2(s)$  with  $r = 5$ .

In practice, control systems are always under the influence of disturbances such as noise. The following example demonstrates how RSMC-IO performs when a disturbance signal in the form of a step function is effective on the output. The system and model given in Eq. (34) are simulated with a relay amplitude of  $r = 20$  and the results are presented in Figure 10. The initial value of the disturbance is zero ( $d = 0$ ). At  $t = 7.5s$  and  $t = 21s$  it takes the values  $d = 0.75$  and  $d = -0.2$ , respectively. The disturbance's effect on the output is clear from Figure 10.a. Figure 10.c shows that at  $t = 7.5s$  the sliding mode conditions are disrupted for an instant,

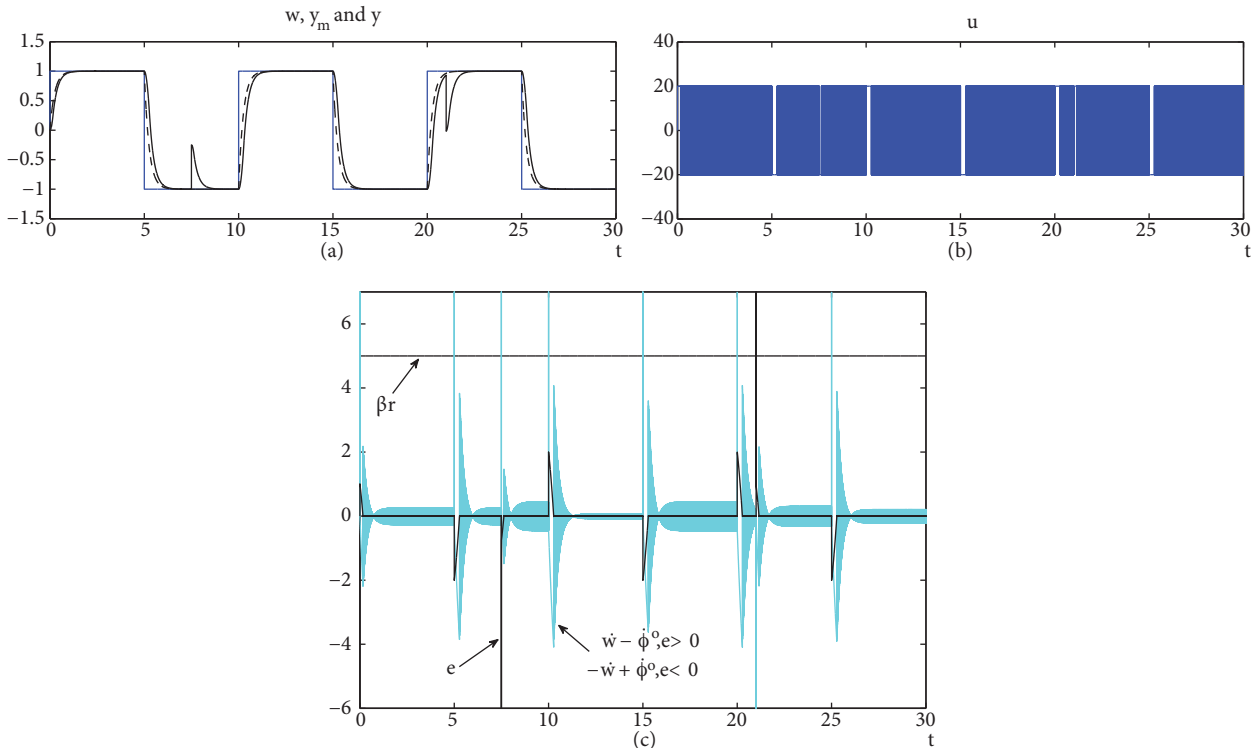


**Figure 10.** Constant additive disturbance. Results for  $G_1(s)$  and  $M_1(s)$  with  $r = 20$ .

but immediately satisfied again. The error, however, is no longer zero due to the disturbance; as a result sliding motion is interrupted. When the error returns to zero the relay continues to operate in sliding motion. On the other hand, the change in the disturbance signal does not disrupt the sliding mode conditions at  $t = 21s$ . As soon as the error returns to zero after a reaching phase, the system continues to operate in sliding mode. Note that when the disturbance jumps to a different value the derivative of the term  $\psi$  in Eq. (23) becomes very large. As a result, the necessary relay amplitude to prevent the relay from leaving sliding mode may be too large to realize in practical applications. Furthermore, the disturbance causes the error to instantly take a value other than zero and a reaching phase follows until it reaches zero again. Therefore, the suggested course of action is to increase the relay amplitude as much as possible in order to shorten the durations of these reaching phases.

Figure 11 presents the results obtained by simulating the system and model in Eq. (34) under the influence of a zero mean additive white noise with variance  $\sigma = 0.01$ . As explained in Section 3.2, the derivatives of the noise are added to the error derivatives, thus making it impossible to satisfy the sliding mode condition (Eq. (20)) with realizably small relay amplitudes. For that reason the model transfer function is modified as below, so that its inverse acts as a low-pass filter to filter out the high frequency components of the noise.

$$M'_1(s) = D(s)M_1(s) = \frac{(0.01s + 1)^2}{0.25s + 1} \tag{38}$$

Because of this change, the relative order condition is no longer satisfied ( $\rho(M_1^{-1}G_1) = 3$ ) over the entire frequency spectrum, but it is still valid in the operating frequency range of the system. Evidentially, sliding mode is achieved and the system output tracks the reference model in the first graph (Figure 11.a). Figure 11.c shows that the unfiltered components of the disturbance appear to be added to the error signal as expected. Recall that the system output is given by  $y = Mw - Me$ . In other words, the error along with the unfiltered components of the noise is filtered by the model and is effective on the output. This can be clearly observed in Figure 11.a.

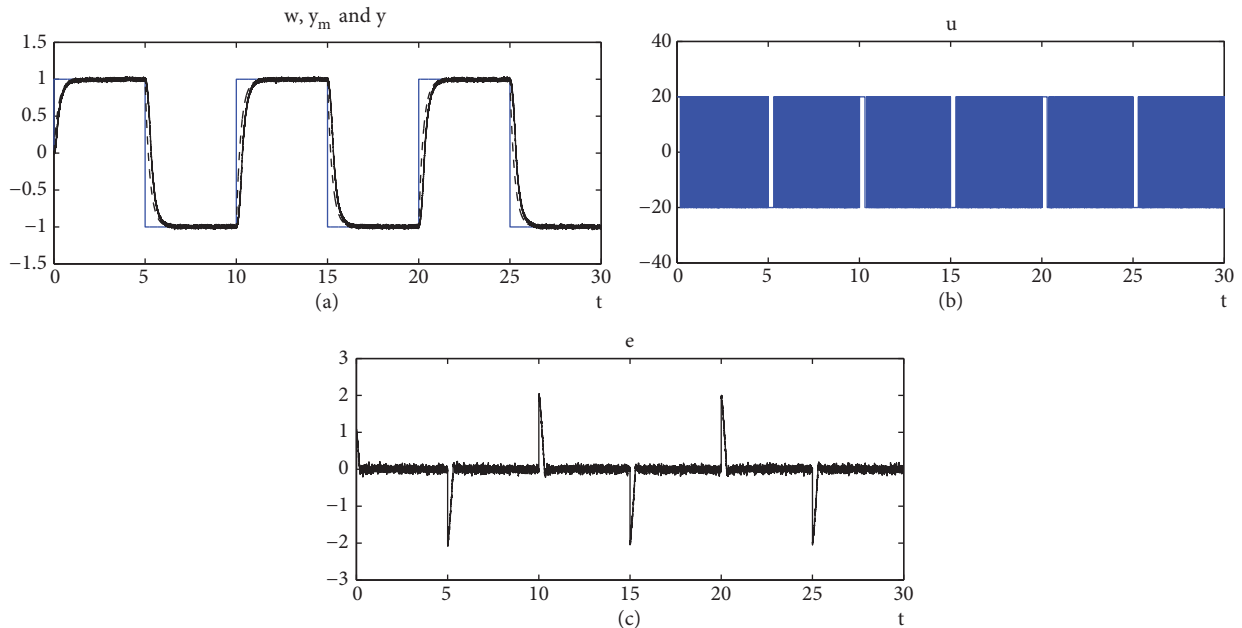


**Figure 11.** Additive white noise. Results for  $G_1(s)$  and  $M_1(s)$  with  $r = 20$ .

Note that the choice of  $D(s)$  is made based on the operating frequency of the controlled system. If the bandwidth of  $1/D(s)$  is too narrow, i.e. close to the system's operating frequency, the relative order condition cannot be satisfied in this frequency range and sliding motion cannot be achieved. If the bandwidth is too wide, on the other hand, the noise signal is not sufficiently filtered and sliding motion does not occur in this case either.

In the following example, the system in Eq. (34) is utilized to examine the effect of measurement noise on the control performance. A high frequency noise originating from the output sensor in the form  $m(t) = 0.05\sin(4000\pi t) + 0.1$  is assumed to be present in the system. The results provided in Figure 12 indicate that, even though the relay element is operating in sliding mode, model following is not achieved due to the measurement error, which is directly added to the system output.

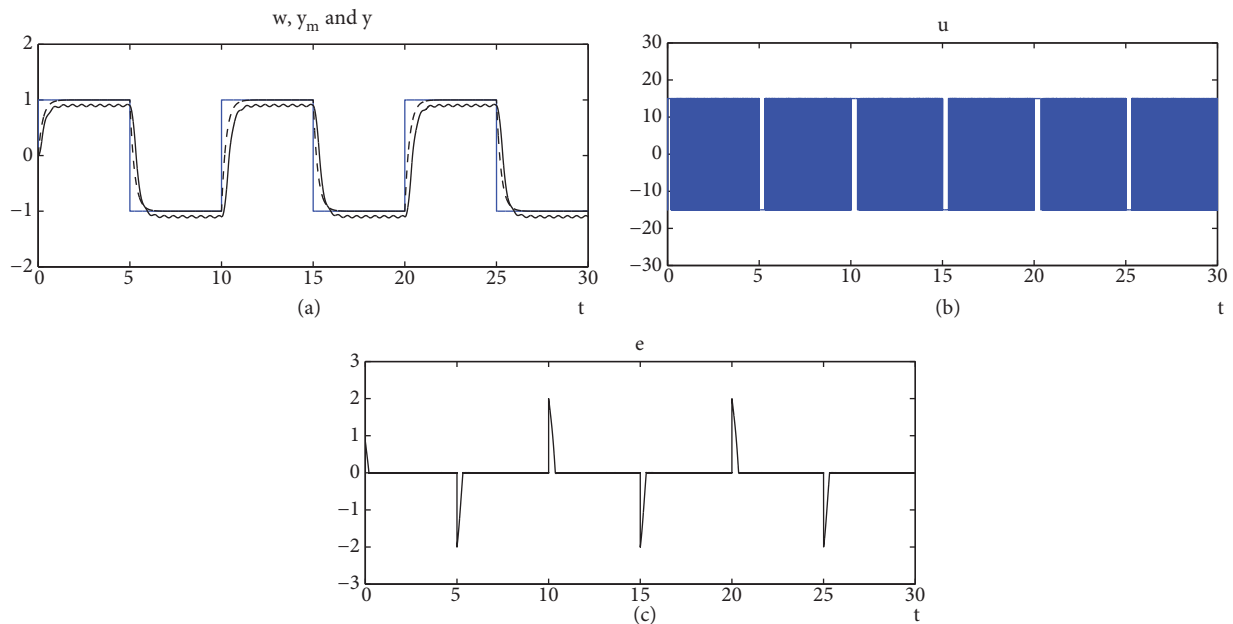


**Figure 12.** Measurement noise. Results for  $G_1(s)$  and  $M_1(s)$  with  $r = 20$ .

## 5. Conclusion

The relay sliding mode control method based on the input-output model has been presented in this paper. Conditions to obtain sliding motion are derived in both ideal and nonideal operating conditions. An extended control structure is introduced to eliminate the chattering problem. Provided theoretical results are then tested extensively via simulations.

The condition for sliding mode can be expressed as a simple inequality. As it is usually not possible to change or modify the system to be controlled, as long as the relative order of the overall open loop system meets a certain condition, the relay amplitude is the decisive parameter for this method. In other words, it is shown that an appropriate relay amplitude is required for sliding motion to occur and the control performance improves as the relay amplitude is increased. However, in practice, physical constraints on the actuator elements may limit the choice of the relay amplitude.

If the system in question does not satisfy the relative order condition, the control structure can be extended by introducing filters of appropriate orders to satisfy this condition. When placed after the relay element, these filters can also be used to obtain a smoother control input rather than the high frequency signal



at the relay output. As a result, not only is chattering reduced, but also the physical constraints limiting the choice of the relay amplitude and sampling period are bypassed.

Analyses involving nonideal operating conditions such as parameter variations and disturbances indicate that a larger relay amplitude needs to be chosen to satisfy the sliding mode condition when compared to the ideal case. An additional precaution has to be taken if a high frequency disturbance such as white noise is effective on the system. The inverse of the model transfer function is modified by introducing a low pass filter to eliminate the high frequency components of the disturbance. Simulations and application results have confirmed that, this way, sliding motion can be achieved with relay amplitudes small enough to be realized in practice. Further, it is shown that RSMC-IO is not robust against measurement noise, a fact that is often disregarded in SMC literature.

In conclusion, RSMC-IO is a simple yet very effective and robust control method. It can be used for the control of both linear and nonlinear systems. It needs only the knowledge of the system's relative order as a priori information; a complete system model is not required.

### References

- [1] Emelyanov SV. Theory of Variable Structure Control Systems, Moscow, Russia: Nauka, 1970.
- [2] Utkin VI. Sliding Modes and Their Applications in Variable Structure Systems, Russia: MIR Publishers, English Translation 1978, 1977.
- [3] [Utkin VI. Variable structure systems with sliding modes. IEEE Transactions on Automatic Control 1977; 22: 212-222.](#)
- [4] Zinober ASI. Variable Structure and Lyapunov Control, London, UK: Springer-Verlag, 1993.
- [5] [Hung JY, Gao W, Hung JC. Variable structure control: a survey. IEEE Transactions on Industrial Electronics 1993; 40: 2-22.](#)
- [6] Edwards C, Spurgeon SK. Sliding Mode Control, Theory and Applications, Vol. 7 of Systems and Control Book Series, UK: Taylor and Francis Ltd., 1998.
- [7] Young KD, Utkin VI, Özgüner Ü. A control engineer's guide to sliding mode control. IEEE Transactions on Automatic Control 1999; 7: 328-342.
- [8] Perruquetti W, Barbot JP. Sliding Mode Control in Engineering, USA: Marcel Dekker, 2002.
- [9] [Bartoszewicz A, Zuk J. Sliding mode control - Basic concepts and current trends. In: IEEE 2010 International Symposium on Industrial Electronics \(ISIE\); Bari, Italy: IEEE. pp. 3772-3777.](#)
- [10] Young KD, Drakunov SV. Sliding mode control with chattering reduction. In: American Control Conference (ACC); 24-26 June 1992; Chicago, IL, USA: pp. 1291-1292.
- [11] [Boiko IM. Analysis of chattering in sliding mode control systems with continuous boundary layer approximation of discontinuous control. In: American Control Conference \(ACC\); June 29 2011-July 1 2011; San Francisco, CA, USA: pp. 757-762.](#)
- [12] Utkin VI, Lee H. Chattering problem in sliding mode control systems. In: International Workshop on Variable Structure Systems, VSS'06; 5-7 June 2006; Alghero, Sardinia, Italy: pp. 346-350.
- [13] [Fridman LM. An averaging approach to chattering. IEEE Transactions on Automatic Control 2001; 46: 1260-1265.](#)
- [14] [Tseng ML, Chen MS. Chattering reduction of sliding mode control by low-pass filtering the control signal. Asian Journal of Control 2010; 12: 392-398.](#)
- [15] [Drakunov SV, Utkin VI. Sliding mode observers - Tutorial. In: Proceedings of the 34th Conference on Decision and Control; 13-15 Dec 1995; New Orleans, LA, USA: 3376-3378.](#)

- [16] Fernando T, Sreeram V, Bandyopadhyay B. Sliding mode functional observers. In: 10th International Conference on Control, Automation, Robotics and Vision; 17-20 Dec. 2008; Hanoi, Vietnam: 1012-1016.
- [17] Bartolini G, Punta E. Sliding mode control based on observers for uncertain nonlinear systems. In: American Control Conference (ACC); 27-29 June 2012; Montreal, QC, Canada: 6178-6183.
- [18] Heck BS, Ferri AA. Application of output feedback in variable structure control systems. *Journal of Guidance, Control and Dynamics* 1989; 12: 932-935.
- [19] White BA. Sliding mode stabilization of uncertain systems using only output information. In: *Deterministic Control of Uncertain Systems*, Ed. Zinober ASI., London, UK: Peter Peregrinus Ltd., 1990.
- [20] Edwards C, Spurgeon SK. Application of output feedback in variable structure control systems. *International Journal of Control* 1995; 62: 1129-1144.
- [21] Demircioğlu H, Gawthrop PJ. Continuous-time relay self-tuning control. *International Journal of Control* 1988; 47: 1061-1080.
- [22] Demircioğlu H. Continuous-time self-tuning algorithms. PhD, University of Glasgow, UK, 1989.
- [23] Demircioğlu H, Özol O. Model dayanıklıkayan kipli denetim ile model dayanaklıuyarlamalıdenetimin karşılaştırılması(in Turkish). In: TOK'2008 Otomatik Kontrol Ulusal Toplantısı; 13-15 November 2008; İstanbul, Turkey: 303-308.
- [24] Yıldız ŞK. Giriş çıkış modeline dayalı rölö ile kayan kipli denetim (in Turkish). PhD, Hacettepe University, Ankara, Turkey, 2013.
- [25] Tsympkin YZ. *Relay Control Systems (English translation)*. UK: Cambridge University Press, 1985.